The impact of N,N-dimethyldodecylamine N-oxide (DDAO) concentration on the crystallisation of sodium dodecyl sulfate (SDS) systems and the resulting changes to viscosity, crystal structure, shape and the kinetics of crystal growth

Emily Summerton[a] (els303@student.bham.ac.uk, +447533301652), Martin J. Hollamby[b] (m.hollamby@keele.ac.uk), Georgina Zimbitas[a] (g.zimbitas@bham.ac.uk), Tim Snow[c] (tim.snow@diamond.ac.uk), Andrew J. Smith[c] (andrew.smith@diamond.ac.uk), Jens Sommertune[d] (jens.sommertune@ri.se), Jeanluc Bettiol[e] (bettiol.j@pg.com), Christopher Jones[e] (jones.cs@pg.com), Melanie M. Britton[f] (m.m.britton@bham.ac.uk), Serafim Bakalis[a,g] (Serafim.Bakalis@nottingham.ac.uk)

[a]School of Chemical Engineering, University of Birmingham, Edgbaston, B152TT, UK
[b]School of Chemistry, University of Keele, Staffordshire, ST5 5BG, UK
[c]Diamond Light Source, Harwell Science and Innovation Campus, Didcot, OX11 0DE, UK
[d]RISE Research Institutes of Sweden, Surfaces, Processes, and Formulation, SE-114 86 Stockholm, Sweden
[e]Procter and Gamble Brussels Innovation Center, Temselaan 100, 1853, Strombeek Bever, Belgium
[f]School of Chemistry, University of Birmingham, Edgbaston, B152TT
[g]Department of Chemical and Environmental Engineering, University of Nottingham, Nottingham, NG7 2RD

Abstract

Hypothesis

At low temperatures stability issues arise in commercial detergent products when surfactant crystallisation occurs, a process which is not currently well-understood. An understanding of the phase transition can be obtained using a simple binary SDS (sodium dodecyl sulfate) + DDAO (N,N-dimethyldodecylamine N-oxide) aqueous system. It expected that the crystallisation temperature of an SDS system can be lowered with addition of DDAO, thus providing a route to improve detergent stability.

Experiments

Detergent systems are typically comprised of anionic surfactants, non-ionic surfactants and water. This study explores the crystallisation of a three component system consisting of sodium dodecyl sulfate (SDS), N,N–dimethyldodecylamine N-oxide (DDAO), and water using wide-angle X-ray scattering (WAXS), differential scanning calorimetry (DSC) and confocal Raman microscopy.

Findings

The presence of DDAO lowered the crystallisation temperature of a 20 wt. % SDS system. For all aqueous mixtures of SDS + DDAO at low temperatures, SDS hydrated crystals, $SDS{\cdot}1/2H_2O$ or $SDS{\cdot}H_2O$, formed. SDS hydrates comprising of layers of SDS separated by water layers. DDAO tended to reside in the vicinity of these

SDS crystals. In the absence of DDAO an additional intermediary hydrate structure, $SDS \cdot 1/8H_2O$, formed whereas for mixed SDS + DDAO systems no such structure was detected during crystallisation.

Keywords: sodium dodecyl sulfate; N,N-dimethyldodecylamine N-oxide; low temperature; crystallization; X-ray scattering; detergent stability

1. Introduction

Home and personal care products are primarily composed of water and surfactants, with the total surfactant concentration ranging from 10 to 50 wt. % [1, 2]. Two surfactants that reside in typical formulations include the anionic surfactant sodium dodecyl sulfate (SDS) [3] and the non-ionic surfactant N,N-dimethyldodecylamine N-oxide (DDAO) [4] (Figure 1). Due to the increasing global demand for these products, the SDS market is growing with an estimated value of $700 million by 2024 [5].

(a)

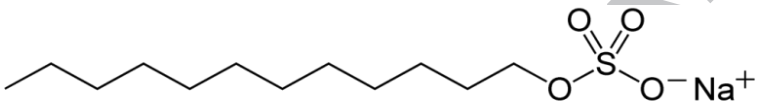

(b)

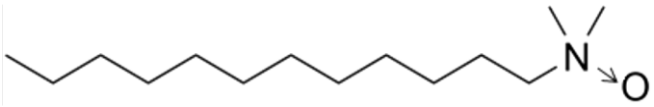

Figure 1. Molecular structure of (a) sodium dodecyl sulfate (SDS) and (b) N,N-dimethyldodecylamine N-oxide (DDAO).

Commercial surfactant systems are used worldwide and therefore needs to be supplied to many different regions, so it must demonstrate chemical and physical stability across a wide temperature range. At ambient temperature, the surfactants in the product aggregate to form mixed micelles. However, upon exposure to low temperatures, surfactant crystallisation may occur in the product. Although the change is reversible and does not affect the performance, the change in appearance makes it unacceptable to consumers. Manufacturers have developed a range of methods to evaluate the stability of formulations at low temperatures, typically involving the storage of formulations at controlled temperature conditions. To improve both product stability and the method for testing for failures, it is critical to understand the crystallisation process.

Despite the industrial significance of SDS and DDAO surfactants, due to their extensive use in detergents products, the crystallisation of mixed SDS + DDAO systems little attention has been received in this area. Smith

et al. considered the crystallisation of the surfactant SDS at concentrations ranging from 5 to 20 wt. % [6, 7]. A decrease in the applied cooling rate was found to increase the temperature of crystallisation and reduce the width of the metastable zone. They also report the structure of anhydrous SDS for the first time and compare the findings to SDS hydrates. More recently, Miller *et al.* observed the effect of different isothermal and non-isothermal conditions on the morphology of crystals forming from a 20 wt. % SDS solution [8, 9]. The temperature and the cooling rate were found to dictate whether the crystals form needles or platelets.

The majority of the literature for the crystallisation of mixed surfactant systems date back to the 1980s and 1990s. The Krafft temperature, T_k, for some binary surfactant mixtures is found to be lower than their respective single components [10]. The decrease in T_k of an anionic surfactant system upon the addition of a second anionic or non-ionic surfactant has been demonstrated for binary surfactant solutions comprising of two different sulfates or sulfonates [11]. Furthermore, the addition of the non-ionic surfactant, nonylphenol ethoxylate, to a solution of SDS caused the precipitation boundary to reduce in size [12]. In these mixed surfactant systems micelle formation becomes increasingly favoured, lowering the CMC and reducing the monomer concentration that is able to form crystals [13].

To the best of our knowledge there is a distinct lack of research into the crystallisation of mixed SDS + DDAO systems, despite its application to commercial products. There are unanswered questions surrounding the influence that DDAO has on SDS crystallisation in terms of the crystallisation kinetics, crystal shape and the structure of the crystals, for which this paper aims to address. In this study SDS and DDAO are present at concentrations typical of those in dish liquid formulations, which are much higher than those previously presented for similar mixed surfactant studies. Crystallisation is initiated by lowering the temperature of the system, in order to replicate conditions that formulations may experience during the supply chain. It is expected that the acquired knowledge from this study will enable industries to gain a greater understanding of the behaviour of their dish liquid formulations at low temperatures. In turn, this will result in improvements to product stability and the accompanying stability test methods.

2. Materials and methods

2.1 Materials

Aqueous surfactant solutions containing 20 wt. % SDS (ionic) and various amounts of the non-ionic surfactant DDAO (0 - 5 wt. %) at pH 9 were used throughout this study. SDS was purchased from Fischer Scientific at a

purity level greater than 97.5 %. DDAO was purchased from Sigma Aldrich in aqueous form at a concentration of 30 wt. %. Both surfactants were used without further purification. All solutions were freshly prepared to minimise deviations due to hydrolysis of SDS. The solution was mixed for 15 minutes at 25 °C and then left for 12 hours to release any entrapped air.

2.2 Methods

2.2.1 Differential scanning calorimetry (DSC)

DSC (Differential scanning calorimetry) thermograms of a pure SDS system and various mixed SDS + DDAO systems were acquired using a Sentaram micro DSC. Distilled water was used as the reference sample. For each run approximately 70 mg of the sample was measured into the sample cell and placed into the DSC furnace chamber.

20 wt. % SDS aqueous solutions, with varying amounts of DDAO (0.5 - 5 wt. %), were cooled and subsequently heated at a rate of 0.1 °C/min. Additionally, a pure 20 wt. % SDS system was cooled across a selection of cooling rates (0.1 - 1 °C/min). The upper temperature was in the range of 30 to 40 °C with the lower limit being −10 °C, at which there was a 20-minute hold time before heating the system. A thermal analysis software package, Calisto processing, was used to acquire enthalpies and peak temperatures from the thermograms.

2.2.2 Confocal Raman microscopy

Confocal Raman microscopy was performed on a WITec alpha 300 system applying a 532 nm excitation laser. Spectra were recorded using a x60 magnification water-immersion objective. The surfactant solutions were applied on a microscopy slide with a recess, with the slide being placed on top of a Linkam PE 94 Peltier cooling stage. A cover slip was placed over the sample and subsequently covered with distilled water which the objective was then immersed into. Typical integration times were in the range of 0.1 s with a resolution of 4 pixels/μm^2. The data was analysed using WITec Project Plus 4.1 software. Cluster analysis followed by de-mixing was subsequently performed in order to distinguish different chemical components. Raman spectra of the pure surfactants were also recorded. This allowed one to plot distribution maps of the components.

2.2.3 X-ray scattering

Small-angle X-ray scattering (SAXS) and wide-angle X-ray scattering (WAXS) data was obtained using the I22 beamline at Diamond Light Source, Oxfordshire, UK. Samples were loaded into 1.8 mm (internal diameter) and

2.0 mm (external diameter) polycarbonate capillaries and mounted in the beam within the Linkam DSC600 capillary stage, which also provided temperature control (at 25 °C and 0 °C, with an applied cooling rate = 19 °C/min). A 12.3989 keV (λ = 0.099987 nm) beam was used with a sample-detector distance of 6702.56 mm, providing a detectable *Q*-range on the SAXS detector of order 0.02 - 2.50 nm^{-1} and 1.51 - 60.57 nm^{-1} on the WAXS detector. Data processing was performed using the DAWN software package [14, 15] and a set of pipelines developed at Diamond Light Source. Before processing uncertainty estimates based on Poisson counting statistics were added to all measurement data, which were subsequently propagated through the image correction steps. Each raw background measurement was corrected for the following: masking pixels, time, incident beam flux, and transmission. Each sample file was corrected for the following: masking pixels, time, incident beam flux, transmission, background, thickness, and scaled to absolute units. The scaling factor for scaling to absolute units was determined using a calibrated glassy carbon sample [16]. After this correction the data was azimuthally averaged, with the resulting uncertainty assuming the largest of: 1) the propagated uncertainties, 2) the standard error of the mean for the data points comprising a bin, or 3) 1% of the mean intensity in the bin. Two-dimensional (2D) plots of the acquired SAXS and WAXs data were displayed as stacked graphs at selected timepoints using OriginPro(v.9.0) graphical software. Time resolved three-dimensional (3D) plots of the WAXS data were produced in MATLAB R2016b.

3. Results and discussion

3.1 Results

3.1.1 Crystallisation temperature

DSC thermograms for the SDS + DDAO systems were acquired upon cooling the system and inducing crystallisation. One main exothermic peak, corresponding to the crystallisation of SDS, was observed for all solutions. Figure 2 shows how the crystallisation temperatures, corresponding to the peak maxima, and the enthalpy of crystallisation, related to the peak area, change with DDAO concentration. Both factors demonstrate strong linear correlation with the amount of DDAO, as anticipated from pre-existing studies [3]. A low cooling rate, 0.1 °C/min, was used since it is representative of typical environmental changes that formulation may experience [8, 9]. There are two types of nucleation, homogenous and heterogenous, and, in most industrial systems, the latter occurs. Here, the DSC cell walls provide a surface from which crystals can nucleate.

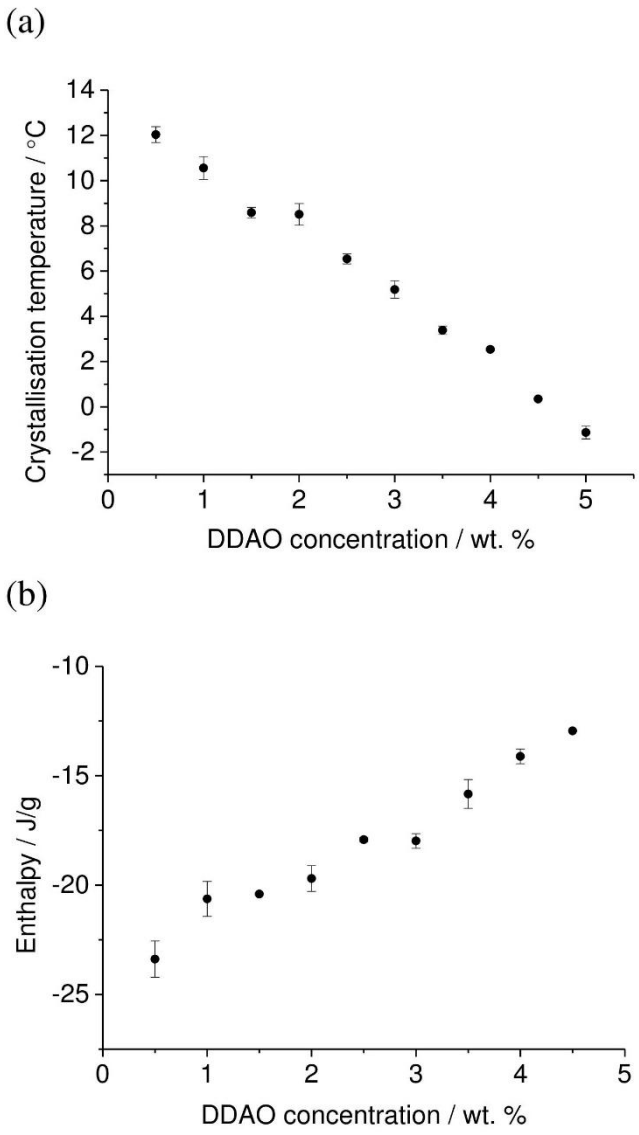

Figure 2. Plots of **(a)** crystallisation temperature and **(b)** enthalpy of crystallisation versus DDAO concentration for SDS + DDAO systems.

It is also important to consider the effect that the cooling rate has on the crystallisation process since formulations can be exposed to various temperature fluctuation. When the cooling rate was varied between 0.1 and 1 °C/min, a change in the crystallisation temperature was observed. The higher the cooling rate, the lower the crystallisation temperature attained from the DSC thermogram (Figure 3).

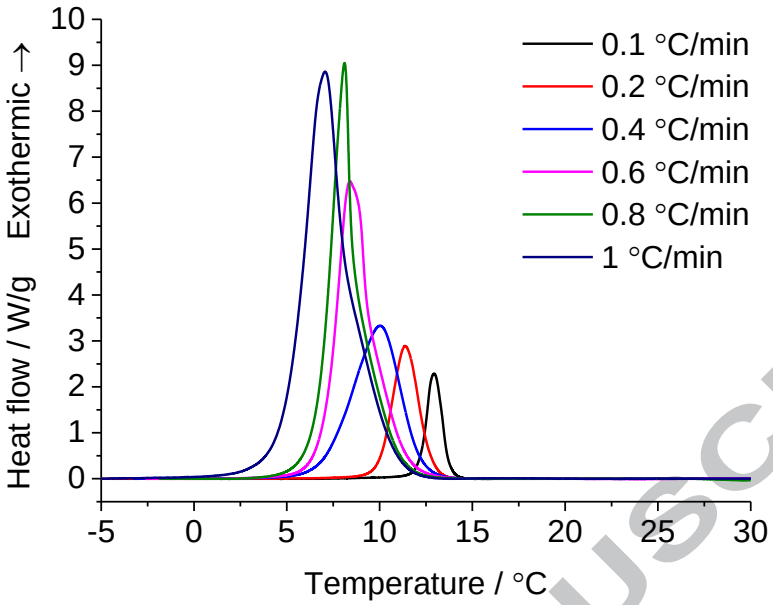

Figure 3. DSC thermograms acquired upon cooling a 20 wt. % SDS system to −5 °C across a range of cooling rates.

3.1.2 Crystal structure and kinetics

3.1.2.1 Crystal Structure

WAXS was used to follow the crystallisation of the pure SDS and SDS + DDAO systems *in situ*. The 2D and 3D WAXS profiles, acquired when holding the systems at 0 °C, are presented in Figure 4.

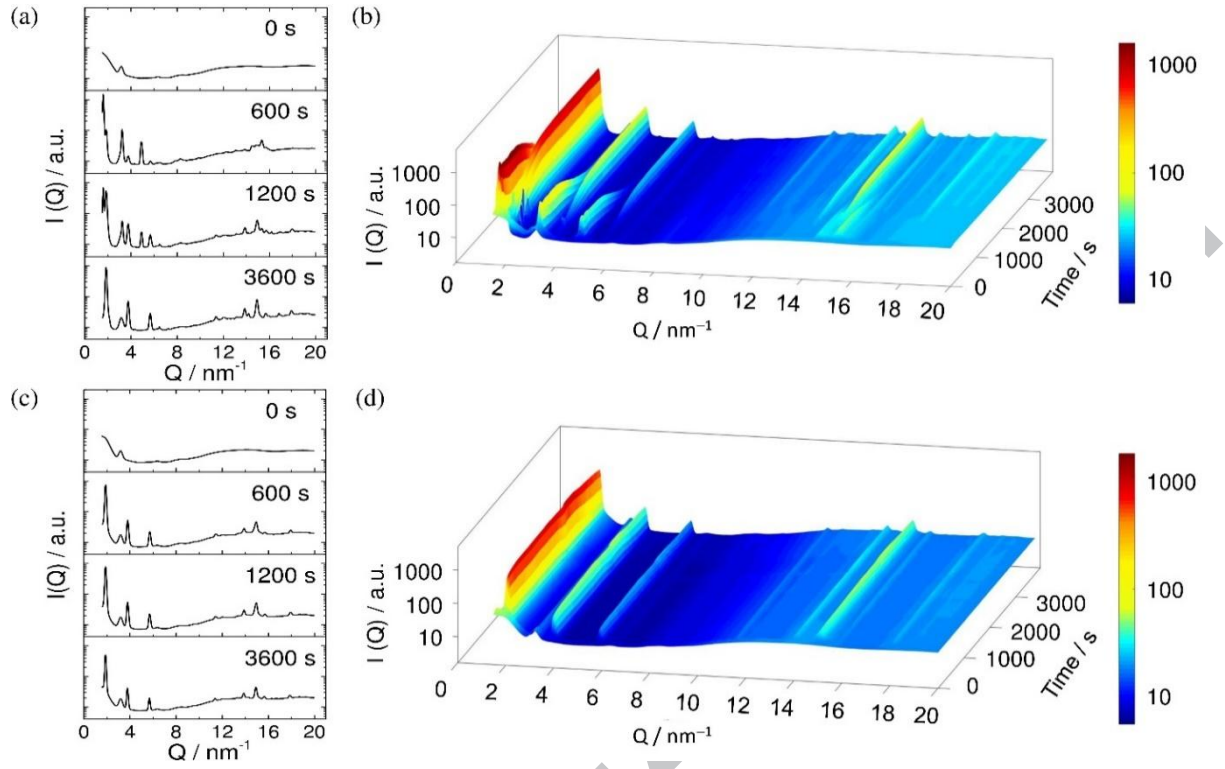

Figure 4. (a) Plot showing the WAXS intensity, I(Q) as a function of Q for selected time points 120 s, 480 s, 1200 s and 2800 s for a 20 wt. % SDS solution held at 0 °C after being cooled from 25 °C at 19 °C /min; **(b)** 3D plot showing the change in I(Q) vs. Q during crystallisation as a function of time for the same 20 wt. % SDS solution; **(c)** Plot showing the WAXS intensity, I(Q) as a function of Q for selected time points 120 s, 480 s, 1200 s and 2800 s for a 20 wt. % SDS + 3 wt. % DDAO solution held at 0 °C after being cooled from 25 °C at 19 °C /min; (d) 3D plot showing the change in I(Q) vs. Q as a function of time during crystallisation for the same 20 wt. % SDS + 3 wt. % DDAO solution. The corresponding plots for 20 wt. % SDS + 1, 2, 4 and 5 wt. % DDAO respectively are provided in Figure S1.

In the pure SDS system, approximately 40 s after reaching 0 °C, a peak initially starts to develop at 1.65 nm^{-1} and the intensity of this peak increases for 20 seconds. This corresponds to a structure with a *d*-spacing of 3.86 ± 0.03 nm. Second and third reflections of this primary peak are visible at 3.24 and 4.91 nm^{-1}. The *d*-spacing values implies a $SDS{\cdot}1/8H_2O$ hydrated crystal [17] [18]. Hydrated SDS crystal structures are comprised of layers of SDS molecules closely aligned to one another, with the SDS layers separated by water-rich regions. The *d*-spacing corresponds to the distance between the SDS layers. Other notable peaks at 14.5, 14.8 and 15.4 nm^{-1} are likely to arise from the spacing between the head-groups and alkyl chains of SDS. The most intense of these is likely to be the head-head peak, which is found to be at 15.4 nm^{-1} (*d* = 0.41 nm).

Approximately 400 s after reaching 0 °C, there is a change in structure, as shown by a reduction in intensity of the peaks at 1.65, 3.24, 4.91, 14.5, 14.8 and 15.4 nm^{-1} and an increase in intensity in peaks at 1.85, 3.76, 5.67, 11.37, 13.89, 14.95, 15.70, 17.96 nm^{-1}. This transition takes approximately 2000 s to complete. The first four peaks are likely to be the 1st, 2nd, 3rd and 6th reflections and the *d*-spacing of structure is 3.32 nm. This value is close to that of the $SDS{\cdot}1/2H_2O$ or $SDS{\cdot}H_2O$ hydrates reported in the literature [17, 18]. The inclusion of more water into the headgroup region results in the alkyl chains becoming tilted, leading to a reduction in the *d*-spacing. The higher *Q* peaks are again likely to arise from the spacing between the head-groups and alkyl chains of SDS. The most intense of these, again likely to be the head-head peak, is now found at 14.95 nm^{-1} (d = 0.42 nm).

In contrast, the WAXS data for the SDS + DDAO systems points to the existence of just one crystal structure throughout the crystallisation process. There are significant peaks detected at 1.88, 3.81, 5.74, 11.48, 13.9, 14.9, 15.7 and 17.9 nm^{-1}, in clear similarity to the data for the second crystalline phase formed by the 20 wt. % SDS solution. As with the 20 wt. % SDS solution, the crystal is therefore likely to be the $SDS{\cdot}1/2H_2O$ or $SDS{\cdot}H_2O$ hydrate, implying no DDAO resides in the crystal.

3.1.2.2 Kinetics of the phase transition

In addition to understanding the structural changes, X-ray scattering can also provide information on the kinetics of the crystallisation process. The primary Bragg peak is detected at 1.9 nm^{-1} in the SAXS profiles for all SDS + DDAO systems. SAXS profiles for the systems are provided in the supplementary information at various timepoints. Figure 5(a) shows the increase in peak intensity as a function of time for 20 wt. % SDS systems with different amounts of added DDAO. Upon increasing the amount of DDAO there are two notable changes in the plot. Firstly, there is an increase in the lag-time until the peak is first observed and, secondly, the rate at which the peak grows decreases in the trend shown in Figure 5(b). The gradient can be related to the rate of growth and the time lag indicates the induction time. The drop in the signal of the 1 wt.% DDAO system after crystallisation may be due to a decline in underlying signal or a change in density.

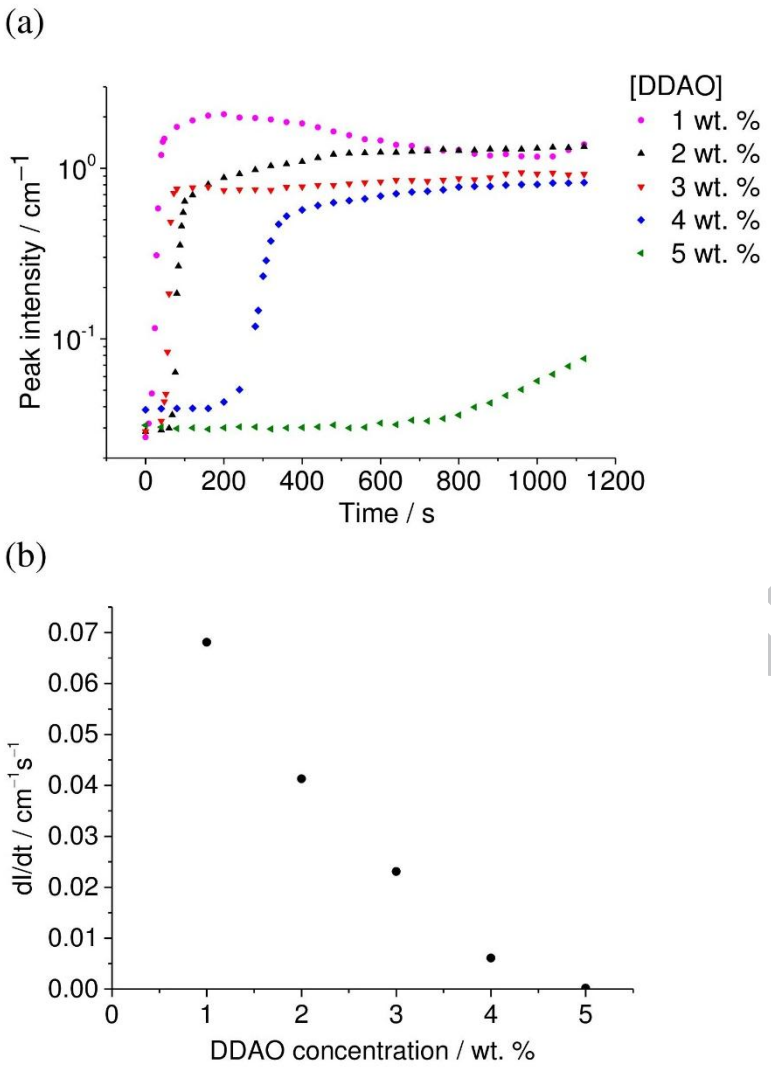

Figure 5. (a) Plot of the change in maximum intensity of the 1st Bragg peak (at 1.9 nm^{-1} in the SAXS) during crystallisation as a function of time for all samples containing DDAO (1 - 5 wt. %); **(b)** Plot showing the rate of change of peak intensity during crystallisation as a function of DDAO concentration.

3.1.3 Crystal shape and growth characteristics

The Raman spectra for the three individual surfactant components are displayed in Figure 6. DDAO can be clearly distinguished from the SDS contributions by the peak above 3000 cm^{-1} and the peak below 800 cm^{-1}. Furthermore, there are two SDS contributions that can be distinguished by their differences in the peak profile around 800 cm^{-1}. The two SDS contributions arise from the orientation of SDS to the laser beam. Although few reports in this area, one study uses Raman spectroscopy to investigate changes observed during SDS crystallisation, including increased peak splitting and an increased degree of trans conformers [19].

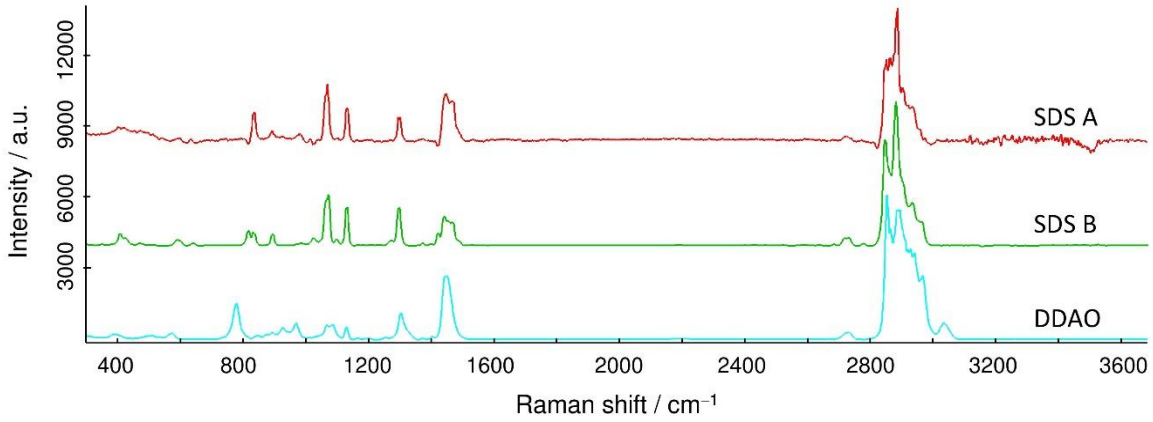

Figure 6. Raman spectra for SDS A (red line), SDS B (green line) and DDAO (blue line); A and B refer to different forms or orientation of the SDS component.

Figure 7 displays confocal Raman microscopy images for crystals formed from 20 wt. % SDS and 20 wt. % + 3 wt. % DDAO solution. In the pure SDS system both SDS contributions are present and exist as platelets, with a considerable number orientated on their side. From Figure 7(b), the crystals initially appear needle-shaped. However, a second image (Figure 7(c)) acquired at a 5 μm height difference, gave a similar profile, indicating the existence of side-on platelets. This is due to local supersaturation at the point of contact between the cooling stage and the surfactant solution, where crystals begin growing upwards.

When DDAO is added, at a level of 3 wt. %, the resultant crystals are ring shaped and grow on a much smaller scale (Figure 7(e)-(g)). Due to the absence of any red-coloured regions, only one SDS contribution exists in the mixed surfactant system. Furthermore, the green-coloured area, corresponding to DDAO, is concentrated in the same region as SDS, implying a tendency of DDAO to surround the SDS crystals.

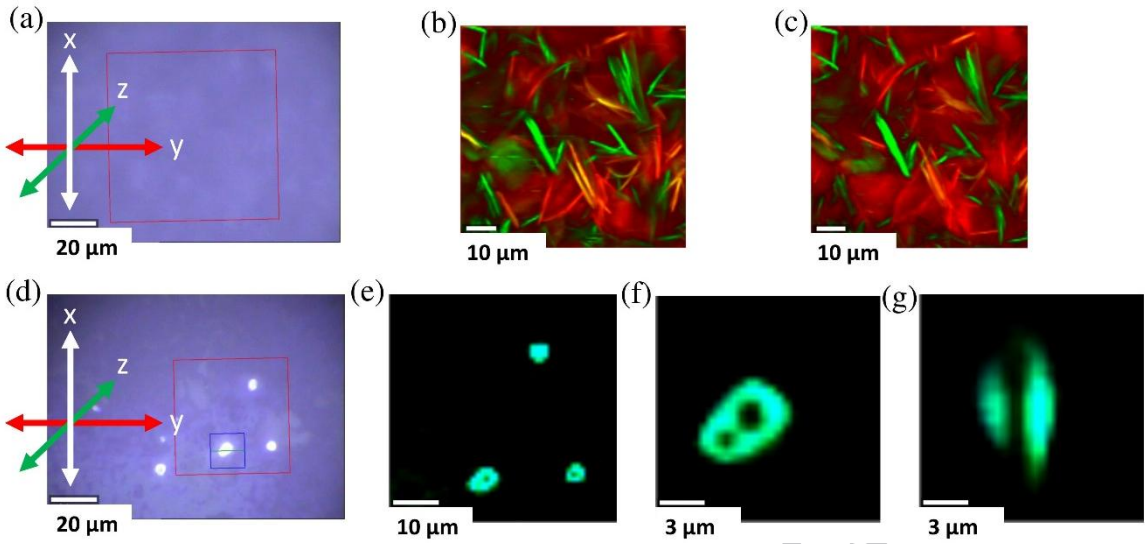

Figure 7. (a) Location selected for the analysis of a crystalline solution of 20 wt. % SDS; **(b)** Confocal scans of the *xy* plane of the red boxed area in (a) with z = 0 µm or **(c)** z = +5 µm; **(d)** Locations selected for the analysis of a crystalline solution of 20 wt. % SDS + 3 wt. % DDAO; **(e)** Confocal scan of the *xy* plane of the red boxed area in (d) with z = 0 µm; **(f)** Confocal scan of the *xy* plane of the blue boxed area in (d) with z = 0 µm; **(g)** Confocal depth scan of the *yz* plane attained by vertically slicing along green line in (d) with z = –7.5 to +7.5 µm.

3.2 Discussion

Non-ideal mixed micelles form in SDS + DDAO systems [20] and the deviation from ideality lowers the critical micelle concentration (CMC), in comparison to that of a pure SDS solution. The existence of DDAO enhances micelle formation in the system, consequently reducing the concentration of SDS monomers, which is the driving force for crystallisation [13, 21, 22]. This increased favourability to form micelles is a result of reduced repulsion energy between the SDS groups in mixed SDS + DDAO micelles, compared to pure SDS micelles. In order for SDS to precipitate out of solution the supersaturation level, S (equation 4), must be greater than 1 [23, 24].

$$S = \frac{a_{DS^-} a_{Na^+}}{K_{sp}}, \text{ where } K_{sp} = a_{DS^-,eqm} a_{Na^+eqm} \qquad (4)$$

where a_{DS^-} and a_{Na^+} are the activities of DS^- and Na^+ in the solution and K_{sp} is the solubility product, which is given by the product of the equilibrium activities of DS^- and Na^+ and exhibits temperature dependency.

Upon addition of DDAO, the temperature must be lowered to induce supersaturation so SDS crystals can form. In addition to reducing the crystallisation temperature, the enthalpy of crystallisation is also found to decrease with increasing DDAO concentration.

Larger, less easily-flowing aggregates [25] form when DDAO is present, compared to a pure SDS system. This, in turn, results in an increase in the viscosity of the system with DDAO concentration. Alongside the effects of a reduced SDS monomer concentration, a high solution viscosity can also hinder SDS crystal growth since it can affect both the growth rate and the crystallisation temperature. The effect of viscosity on crystal growth has been reported in a previous study [21] in which ice crystallisation was inhibited when contained within an ultra-viscous solution. In the pure SDS system the viscosity is low and molecular mobility is not restricted. Crystal growth is fast and spreads through the solution, forming many platelets. The mixed 20 wt. % SDS + 3 wt. % DDAO system, being at a higher viscosity, demonstrates slower growth. There is a resultant tendency for crystals to dissolve from the centre, forming ring-shaped crystals [26]. Furthermore, the DDAO surfactant surrounds the SDS crystals which also contributes to the reduced rate of growth. Further insight into how DDAO concentration influences the rate of crystallisation and induction time can also be obtained from the time resolved plots of the intensity of the first Bragg peak in the SAXS profiles. The time lapsed until the peak begins to grow and the gradient of the peak growth correspond to the induction time and rate, respectively. As to be expected, the rate of crystal formation decreases and the time to crystallisation increases with an increase in the amount of DDAO.

Aside from DDAO affecting the crystallisation temperature, rate of formation, shape and viscosity, this non-ionic surfactant also influences the structural changes that occur during SDS crystal formation at 0 °C. The crystals formed from both SDS and SDS + DDAO systems are SDS hydrates, composed of SDS-rich layers separated by water layers, with the ratio of water to SDS varying between the different possible hydrates. WAXS data acquired from SDS + DDAO systems points to the crystal structure being either the SDS·1/2H_2O or SDS·H_2O hydrate, which matches the final structure formed from a pure SDS sample. However, the pure SDS system initially forms the SDS·1/8H_2O hydrate, which then gradually transitions to the SDS·1/2H_2O or SDS·H_2O hydrate. When DDAO is present, SDS is trapped in micelles for a longer period of time. Such a feature is responsible for more controlled crystal growth in the SDS + DDAO system, enabling the final structure to form directly rather than proceeding via an intermediary. Furthermore, confocal Raman microscopy investigations

indicate that, upon SDS crystal formation, DDAO is concentrated on the surface of the SDS crystals where it is able to influence both the mechanism and rate of formation.

4. Conclusions

Increasing the amount of DDAO lowers the concentration of SDS monomers, due to mixed micelle formation, and consequently reduces the drive for SDS crystallisation. In the presence of DDAO, the crystallisation temperature is lowered, compared to that of a pure SDS system. Furthermore, the presence of DDAO was found to significantly increase the induction time to crystallisation, as well as reduce the rate of crystal growth. In the final part of the study, X-ray scattering techniques demonstrate the structural differences and similarities between those of a pure SDS system versus a SDS + DDAO system. Both systems result in the same final structure, where the *d*-spacing and peak assignments are matched to those of $SDS{\cdot}1/2H_2O$ or $SDS{\cdot}H_2O$ hydrate structures, comprised of layers of SDS separated by water layers. The pure SDS system proceeds via the $SDS{\cdot}1/8H_2O$ hydrate structure but, conversely, this intermediary is not detected in the mixed system. DDAO surrounds the crystals and consequently affects the mechanism of their formation.

Through this work a detailed insight has been gained into the nature of the SDS crystallisation process occurring in SDS + DDAO systems under low temperature conditions. SDS and DDAO were chosen as the core surfactants for this study due to their extensive use in industry, especially in dish liquid formulations. It is important to reiterate that, in this study, both surfactants are at concentrations typical of commercial detergent products. DDAO was found to influence the crystallisation temperature, crystal shape, structure and kinetics of SDS solutions. The reported results have furthered the understanding of dish liquid systems at low temperatures, which is important when improving the stability of such formulations. Future work would involve applying the understanding to other surfactant systems of significance in the detergent industry, such as those containing dimethyl laurylaminoacetate betaine and branched sulfated surfactants.

5. Acknowledgements

We would like to gratefully acknowledge the Engineering and Physical Sciences Council and P&G for their financial support (Grant Reference EP/G036713/1). We also acknowledge Diamond Light Source for the award of SAXS/WAXS beamtime on beamline I22 under proposal SM16560. We also thank the RISE institute in

Stockholm that allowed confocal Raman microscopy to be performed. We express gratitude to Dr. Thomas Moxon for producing the MATLAB code for the 3D WAXS profiles.

5. References

1. Summerton, E., et al., *Low temperature stability of surfactant systems.* Trends in Food Science & Technology, 2017. **60**: p. 23-30.
2. Lai, K.Y., *Liquid Detergents*. 1996: CRC Press.
3. Summerton, E., et al., *Crystallisation of sodium dodecyl sulfate and the corresponding effect of 1-dodecanol addition.* Journal of Crystal Growth, 2016. **455:** p. 111-116
4. Búcsi, A., et al., *Determination of pKa of N-alkyl-N,N-dimethylamine-N-oxides using ^{1}H NMR and ^{13}C NMR spectroscopy.* Chemical Papers, 2014. **68**(6): p. 842-846.
5. *Sodium Lauryl Sulfate (SLS) Market to exceed $700 Million by 2024*. Global Market Insights, Inc 2017; Available from: https://globenewswire.com/news-release/2017/04/24/970119/0/en/Sodium-Lauryl-Sulfate-SLS-Market-to-exceed-700-Million-by-2024-Global-Market-Insights-Inc.html.[Accessed 17/05/2018]
6. Smith, L.A., et al., *An examination of the solution phase and nucleation properties of sodium, potassium and rubidium dodecyl sulphates.* Journal of Crystal Growth, 2001. **226**: p. 158-167.
7. Smith, L.A., et al., *Determination of the crystal structure of anhydrous sodium dodecyl sulphate using a combination of synchrotron radiation powder diffraction and molecular modelling techniques.* Journal of Molecular Structure, 2000. **554**: p. 173-182.
8. Miller, R.M., et al., *Isothermal Crystallization Kinetics of Sodium Dodecyl Sulfate–Water Micellar Solutions.* Crystal Growth and Design, 2016. **16**: p. 3379-3388.
9. Miller, R.M., et al., *Crystallization of Sodium Dodecyl Sulfate–Water Micellar Solutions under Linear Cooling*. Crystal Growth and Design, 2017. **17**: p. 2428-2437.
10. Rodriguez, C.H. and J.F. Scamehorn, *Modification of Krafft temperature or solubility of surfactants using surfactant mixtures.* Journal of Surfactants and Detergents, 1999. **2**: p. 17-28.
11. Tsujii, K., N. Saito, and T. Takeuchi, *Krafft points of anionic surfactants and their mixtures with special attention to their applicability in hard water.* Journal of Physical Chemistry, 1980. **84**: p. 2287-2291.

12. Shiau, B.J., J.H. Harwell, and J.F. Scamehorn, *Precipitation of mixtures of anionic and cationic surfactants. 3. Effect of added nonionic surfactant.* Journal of Colloid and Interface Science, 1994. **167**: p. 332-345.

13. Soontravanich, S. and J.F. Scamehorn, *Use of a Nonionic Surfactant to Inhibit Precipitation of Anionic Surfactants by Calcium.* Journal of Surfactants and Detergents, 2009. **13**: p. 13.

14. van der Veen, J.F., *JSR - XFELs, DLSRs and beamline articles.* Journal of Synchrotron Radiation, 2015. **22**: p. 1-2.

15. Filik, J., et al., *Processing two-dimensional X-ray diffraction and small-angle scattering data in DAWN 2.* Journal of Applied Crystallography, 2017. **50**: p. 959-966.

16. Zhang, F., et al., *Glassy Carbon as an Absolute Intensity Calibration Standard for Small-Angle Scattering.* Metallurgical and Materials Transactions A, 2010. **41**: p. 1151-1158.

17. Coiro, V.M., et al., *Structure of a triclinic phase of sodium dodecyl sulfate monohydrate. A comparison with other sodium dodecyl sulfate crystal phases.* Acta Crystallographica Section C, 1987. **43**: p. 850-854.

18. Smith, L.A., et al., *Crystallisation of sodium dodecyl sulphate from aqueous solution: phase identification, crystal morphology, surface chemistry and kinetic interface roughening.* Journal of Crystal Growth, 2004. **263**: p. 480-490.

19. Picquart, M., *Vibrational-mode behavior of SDS aqueous solutions studied by Raman scattering.* Journal of Physical Chemistry, 1986. **90**: p. 243-250.

20. Scamehorn, J.F., *An Overview of Phenomena Involving Surfactant Mixtures.* ACS Symposium Series, 1986. **311**: p. 1-27.

21. Stellner, K.L. and J.F. Scamehorn, *Hardness tolerance of anionic surfactant solutions. 2. Effect of added nonionic surfactant.* Langmuir, 1989. **5**: p. 77-84.

22. Stellner, K.L. and J.F. Scamehorn, *Surfactant precipitation in aqueous-solutions containing mixtures of anionic and nonionic surfactants.* Journal of the American Oil Chemists Society, 1986. **63**: p. 566-574.

23. Soontravanich, S., *Formation and Dissolution of Surfactant Precipitates*. 2007: PhD Thesis, University of Oklahoma.

24. Thanh, N.T.K., N. Maclean, and S. Mahiddine, *Mechanisms of Nucleation and Growth of Nanoparticles in Solution.* Chemical Reviews, 2014. **114**: p. 7610-7630.

25. Akbas, H. and T. Sidim, *The viscous properties of anionic/cationic and cationic/nonionic mixed surfactant systems.* Colloid Journal, 2005. **67**: p. 525-530.

26. Mandal, P.K., et al., *Ring crystals of oligonucleotides: Growth stages and X-ray diffraction studies.* Journal of Crystal Growth, 2012. **354**: p. 20-26.

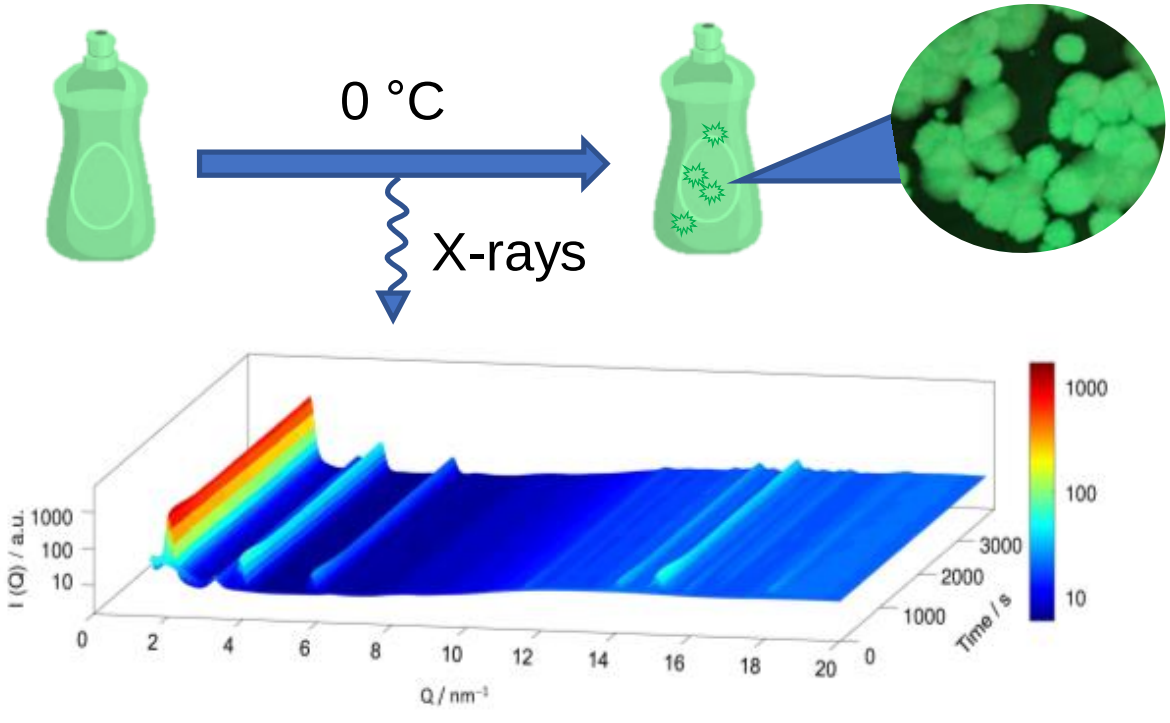
0 °C
X-rays
I (Q) / a.u.
1000
100
10
0
2
4
6
8
10
12
14
16
18
20
Q / nm⁻¹
0
1000
2000
3000
Time / s
1000
100
10